Two-Dimensional Layered Organic−Inorganic Hybrid Perovskite Thin-Film Fabrication by Langmuir−Blodgett and Intercalation Techniques

Yasuhiro F. Miura,* Yoshiya Akagi, Daizo Hishida, and Yuko Takeoka

Read Online

ACCESS | Metrics & More | Article Recommendations | Supporting Information

ABSTRACT: We demonstrate the formation of a well-organized thin film of two-dimensional (2D) layered $(C_{18}H_{37}NH_3)_2PbI_4$ hybrid perovskite by immersing octadecyl amine (ODA) Langmuir−Blodgett (LB) films in an aqueous solution of PbI_2/HI. The immersed films exhibit a sharp absorption band at 486 nm (2.55 eV), which is assigned to the excitonic absorption. The film exhibits a bright green emission under ultraviolet light at room temperature. The photoluminescence spectrum has a distinct peak at 497 nm (2.49 eV) and is a mirror image of the absorption spectrum. X-ray diffraction (XRD) analyses reveal that the film has a bilayer-like structure with a d-spacing of 6.4 nm, which is equal to that of a $(C_{18}H_{37}NH_3)_2PbI_4$ perovskite single crystal with a quantum well (QW) structure. Only intense peaks of the (0 0 l) (l = 2, 4, 6, 8, 10, 12, 14, 16, 18, 20, 22, and 24) reflections are observed in the out-of-plane XRD pattern, indicating that the c axis is vertically oriented with respect to the substrate surface, and the orientational order is remarkably high. Fourier transform infrared spectroscopy reveals that the ODA molecules are protonated in the PbI_2/HI solution. These results suggest that the nitrogen atoms of the ODA molecules in the film are protonated in the PbI_2/HI solution, and then, inorganic layers of the PbI_6 octahedra are intercalated in the alkyl ammonium film to neutralize the positive charge and form a QW structure. Fluorescence microscopy observation reveals that the 2D layered $(C_{18}H_{37}NH_3)_2PbI_4$ film has a relatively uniform surface, reflecting the well-organized layered structure of the base material (ODA LB film). Because the intercalation process can be applied to various metal cations and halogen anions, we believe that the proposed technique will aid in the development of highly efficient 2D layered organic−inorganic hybrid perovskite materials.
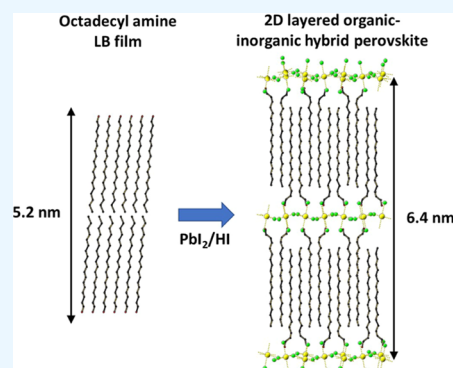
1. INTRODUCTION

Considerable attention has been paid to the development of organic−inorganic hybrid perovskites for various applications—such as solar cells (SCs),[1] light-emitting diodes,[2] photodetectors,[3] X-ray detectors,[4,5] lasers,[6] and thermoelectric devices[7,8]—because of their outstanding properties.

Among them, two-dimensional (2D) layered organic−inorganic hybrid perovskites are currently under spotlight owing to the excellent tunability of their electronic and opto-electronic properties.[9−11] Furthermore, the chemical stability of these 2D materials, especially under moisture, is also a great asset.[12−14] Most of the known 2D perovskite derivatives have additional ammonium or diammonium cations and are represented by the general formula $(R-NH_3)_2MX_4$ or $(NH_3-R-NH_3)MX_4$. This formula is different from that of the 3D perovskites, which are represented by AMX_3 (A = organic cation, M = metal cation, and X = halogen anion).[10] In 3D perovskites, organic cations (A) fill the voids between the metal halide octahedra, resulting in certain restrictions on their sizes and shapes. In contrast, in 2D layered organic−inorganic hybrid perovskite materials, bulky cations with various sizes and shapes can be introduced to tune the properties of these

materials. In such cases, 2D layers of organic cations and those of metal halide octahedra are alternately stacked to form quantum well (QW) superlattices.[9]

Various intrinsic properties, such as exciton dynamics, electronic transport, and electron−phonon coupling, influence the performance of the devices based on 2D layered organic−inorganic hybrid perovskite materials. Therefore, fundamental research is essential to open possibilities for a variety of applications, as mentioned before.[1−8] Although the incorporation of bulky cations, such as in SCs, sometimes limits the performance of the devices, the protection of the ionic lattice of the inorganic octahedra is a major advantage of 2D layered materials. In fact, currently, the fabrication of 2D/3D perovskite hybrid structures is attracting significant attention

because such a structure combines the advantages of both the components.[14,15]

Following the pioneering work of Dolzhenko et al.[16] on the synthesis of single crystals of a 2D layered organic−inorganic hybrid $(C_nH_{2n+1}NH_3)_2PbI_4$ perovskite ($n = 9$), bulk single crystals with $n = 4, 6, 8, 10,$ and 12 have been synthesized, and the exciton states of the 2D materials have been extensively studied.[17,18] Bulk single crystals with larger n values ($n = 14, 16, 18$) have also been studied.[19,20] In the single crystals fabricated via self-organization, the interfaces between the inorganic and organic layers are inherently even. Therefore, 2D layered organic−inorganic hybrid $(C_nH_{2n+1}NH_3)_2PbI_4$ perovskites with naturally formed QW superlattices are considered to be ideal 2D systems, wherein the exudation of the wave function into the adjacent layers is completely suppressed.[21,22] Notably, in many cases, device applications require thin-film fabrications, where solution processes such as spin coating and inkjet printing have certain advantages over other methods in terms of manufacturing cost and possible applications in flexible electronics. Therefore, the fabrication of 2D layered organic−inorganic hybrid perovskite thin films is of paramount importance.

To date, several techniques for the fabrication of thin films of 2D layered organic−inorganic hybrid perovskite materials have been reported. Liang et al.[23] proposed a two-step dipping technique, in which thin films of metal halides are dipped into an organic solution of ammonium iodide; the inorganic thin films can be fabricated by either vacuum evaporation or spin coating. This technique is suitable for intercalating relatively small organic cations into lead halides. However, in general, its application to bulky cations with longer alkyl chains is not straightforward because of the limitation of void sizes in the inorganic base materials. Takeoka et al.[24] fabricated thin films of the 2D layered organic−inorganic hybrid $(NH_3(CH_2)_{12}NH_3)PbBr_4$ perovskite in reverse order. First, the thin films of $NH_3Br(CH_2)_{12}NH_3Br$ were fabricated by spin coating. Next, the organic films were immersed in a solution of lead bromide to achieve intercalation. Intercalation procedures are a versatile technique for fabricating 2D layered organic−inorganic hybrid perovskite thin films and facilitate the variation of the organic and inorganic components.

Nonetheless, there are certain problems that should be overcome; for instance, films fabricated using solution processes tend to exhibit a certain surface roughness with disorders such as grain boundaries and/or defects. Furthermore, different crystallographic phases tend to coexist in the thin-film systems.[12] For instance, a spin-coated thin film of a 2D layered organic−inorganic $(C_{14}H_{29}NH_3)_2PbI_4$ hybrid perovskite exhibited absorption and photoluminescence (PL) emission spectra with two unresolved peaks because of the coexistence of two different crystallographic phases.[12,19] Therefore, a suitable method is required for the fabrication of homogeneous thin films of 2D layered organic−inorganic hybrid perovskites.

The Langmuir−Blodgett (LB) technique is powerful and can assemble organic molecules into tailored 2D molecular sheets. Furthermore, long-chain alkyl ammonium salts are well known as useful building blocks for constructing high-quality LB films.[25−28] Era and Oka demonstrated the fabrication of thin films of 2D layered PbBr- and PbI-based hybrid perovskites.[27,28] First, a monolayer of docosyl ammonium bromide was formed on a special aqueous subphase containing $PbBr_2$ (or PbI_2) and methylammonium bromide (or iodide).

Next, the layer was sequentially transferred onto a solid substrate using the LB technique to build multilayered structures.[27,28] Era and Oka further proposed a method to prepare LB films of a different 2D layered PbBr hybrid perovskite. In this method, an asymmetric bilayer-like film is formed on the aqueous subphase, wherein the PbBr octahedra are sandwiched between the monolayers of docosyl ammonium and hexadecyl ammonium. Next, the floating layer is sequentially transferred onto a solid substrate to form the LB multilayer.[29] Despite the sophistication of these techniques, their application is limited to a narrower range of compositions. For instance, when the hydrophilicity of a molecule exceeds a certain level, the floating layer with the bilayer-like unit tends to dissolve in the aqueous subphase upon compression. Furthermore, in general, the transfer ratios of the floating layers to the solid substrates are sensitive to various conditions, such as pH, temperature, and ions of the subphase.[30] Because different molecular species show different sensitivities to these subphase parameters, these techniques cannot be straightforwardly applied to various molecular systems.

An alternative solution to overcome these problems might be to start from the LB films of alkyl amines instead of those of the alkyl ammonium salts because the method for fabricating LB films of alkyl amines is well established. Takahashi et al.[31] reported that organic molecules of some species can be intercalated in the LB film of octadecyl amine (ODA). Honda et al.[32] suggested that lead iodide octahedra can be intercalated in the ODA LB film to form a thin film of 2D layered organic−inorganic hybrid perovskites; however, the layered structure of the film was not elucidated.

Figure 1 shows the lengths of the c axes for bulk single crystals of 2D layered organic−inorganic $(C_nH_{2n+1}NH_3)_2PbI_4$ ($n = 4, 6, 8, 9, 10, 12, 14, 16,$ and 18) hybrid perovskites plotted against the number of carbon atoms in the alkyl ammonium chain (closed circles). The single crystals have layers of lead iodide octahedra separated by those of the alkyl ammonium chains, forming QW structures.[16−20] The crystal
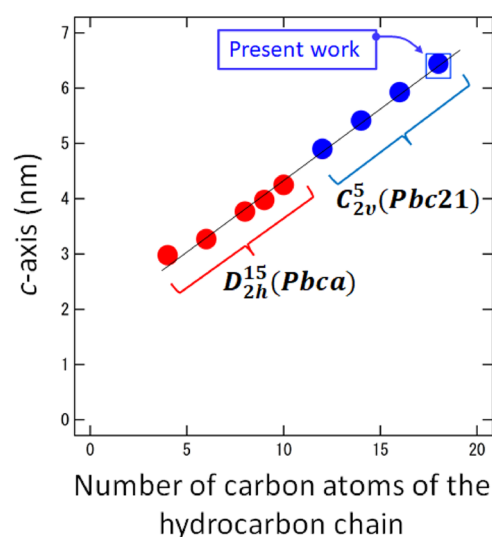
Figure 1. Length of the c axis plotted against the number of carbon atoms along alkyl ammonium chains for bulk crystals of 2D layered organic−inorganic $(C_nH_{2n+1}NH_3)_2PbI_4$ ($n = 4, 6, 8, 9, 10, 12, 14, 16,$ and 18) hybrid perovskites (closed circles). The d-spacing of the prepared thin film is depicted as an open square for comparison.

systems are orthorhombic (space group type: *Pbca* or *Pbc21*), and the unit cell has a bilayer-type structure (interlayer spacing of the sheets of lead iodide octahedra is one half of the *c* axis length). The length of the *c* axis increases linearly with the number of carbon atoms, as shown in Figure 1 (although the crystals are known to undergo structural transitions from orthorhombic to monoclinic structures at higher temperatures, they are not included in Figure 1[19]). Therefore, the development of a versatile technique for fabricating organized thin films of 2D layered hybrid perovskites necessitates the acquisition of a powerful tool to control the interlayer spacing to tune the electronic and opto-electronic properties of thin-film systems.

We demonstrate that a well-organized thin film of the 2D layered organic–inorganic $(C_{18}H_{37}NH_3)_2$ PbI_4 hybrid perovskite can be fabricated by immersing the ODA LB film in a PbI_2/HI solution. The structures and optical properties of the fabricated films were investigated using X-ray diffraction (XRD), ultraviolet (UV)–visible absorption spectroscopy, fluorescence spectroscopy, Fourier transform infrared (FT-IR) spectroscopy, and fluorescence microscopy. The characterization results confirmed that the nitrogen atoms of the ODA LB film were protonated and that the inorganic layers of the lead iodide octahedra were intercalated in the film to neutralize the positive charge. Furthermore, the 2D layered organic–inorganic $(C_{18}H_{37}NH_3)_2PbI_4$ hybrid perovskite contained one single crystallographic phase, whereas different polymorphs tend to coexist in the thin-film systems fabricated by conventional solution processes such as spin coating.[12] Our analyses reveal that the structure of the fabricated 2D layered organic–inorganic $(C_{18}H_{37}NH_3)_2PbI_4$ hybrid perovskite film is equivalent to that of a single crystal of the 2D layered organic–inorganic $(C_{18}H_{37}NH_3)_2PbI_4$ hybrid perovskite and that the orientational order is remarkably high. Furthermore, fluorescence microscopy revealed the uniformity of the film surface observing a step structure created in the film. We believe that the present work will give impetus to research in this field and promote practical applications of these materials.
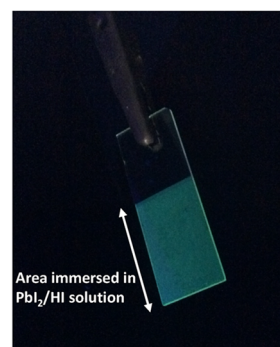
2. RESULTS AND DISCUSSION

Figure 2a shows the UV–visible absorption spectra of the ODA LB film with 21 layers deposited on both sides of the glass substrate, after immersing it in the PbI_2/HI (0.5 mM/1.0 mM) solution for 1–50 min. After the immersion, the transparent ODA LB film gradually turns yellow. As shown in Figure 2a, a distinct absorption band emerges at 486 nm (2.55 eV), and its absorbance increases with time (see also the inset of Figure 2a). After 50 min of immersion, the absorbance reaches 0.91.

Figure 2b depicts a photograph of the 21-layered ODA LB film after immersion in the aqueous PbI_2/HI solution for 50 min under UV irradiation (365 nm). Evidently, the immersed area exhibits a bright green emission at room temperature (the movie is available in the MP4 format in the Supporting Information). Figure 2c shows a typical PL spectrum of the film; the absorption spectrum is also shown for comparison. The PL spectrum has a distinct peak at 497 nm (2.49 eV) and is a mirror image of the absorption spectrum, as shown in Figure 2c.
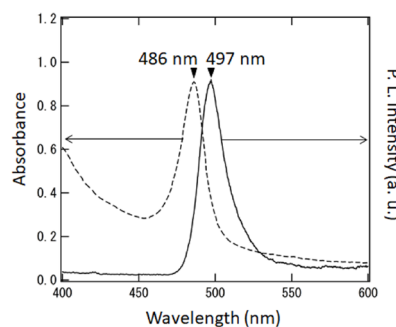
Previously, Ishihara et al.[18] reported the existence of a common sharp absorption band located at 2.56 eV together with a step-like absorption starting at ~2.88 eV for a series of bulk single crystals of $(C_nH_{2n+1}NH_3)_2PbI_4$ perovskites (n = 4,
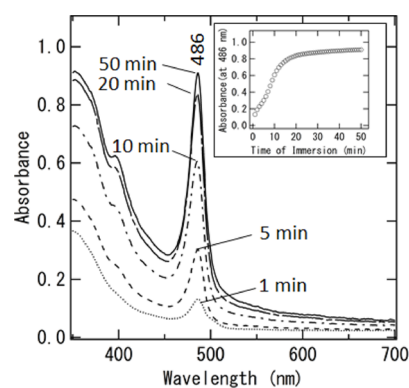

(a)

(b)

(c)

Figure 2. (a) UV–visible absorption spectra of the ODA LB film with 21 layers deposited on both sides of a glass substrate after immersing it in an aqueous PbI_2/HI (0.5 mM/1.0 mM) solution for 1–50 min. The inset shows the peak absorbance at 486 nm plotted against the durations for which the LB film was immersed in the PbI_2/HI solution. (b) Photograph of the LB film with 21 layers, deposited on a glass substrate, obtained under UV radiation (365 nm). (c) Typical PL spectrum of the 21-layered LB film after immersion in the aqueous PbI_2/HI (0.5 mM/1.0 mM) solution for 50 min (solid line). The excitation wavelength was 350 nm. The UV–visible absorption spectrum is shown by a dashed line for comparison.

9, 10, and 12). For our sample, the distinct peak located at 486 nm coincides well with the band reported for the relevant single crystals together with the increase in absorption starting at ~440 nm (2.8 eV).[18] Thus, the sharp absorption at 486 nm (2.55 eV), observed in our study, can be ascribed to the excitonic band, whereas the absorption starting at ~440 nm can be considered to be the absorption edge of the $(C_{18}H_{37}NH_3)_2PbI_4$ perovskite semiconductor. Further, the

(a)

(b)

(c)
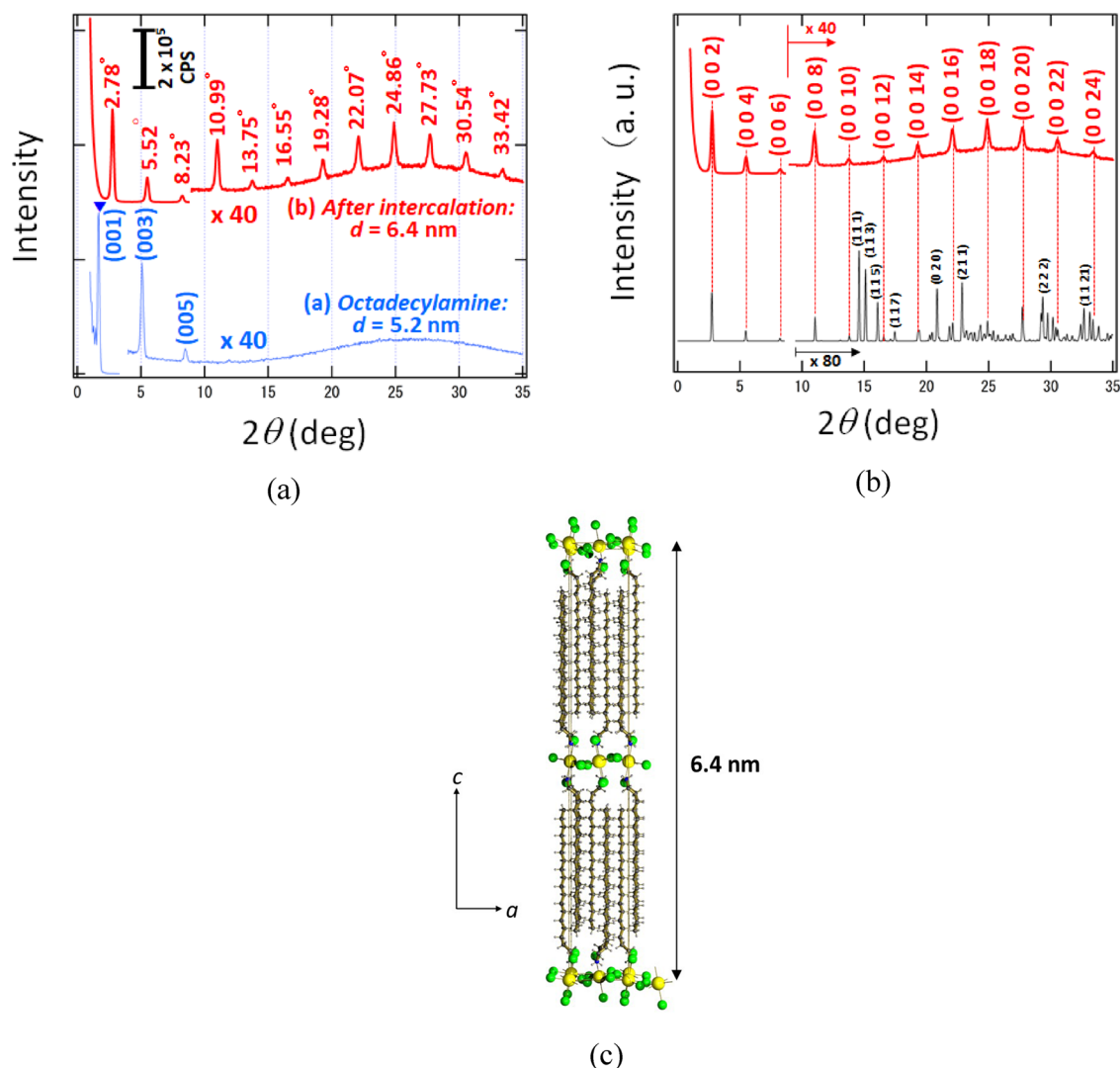
Figure 3. (a) Out-of-plane XRD profiles of the 21-layered ODA LB film before and after immersion in the aqueous PbI_2/HI (0.5 mM/1.0 mM) solution for 50 min. The intensity data for the as-deposited ODA LB film are magnified 40 times for $4° < 2\theta$. The data for the LB film after immersion are magnified 40 times for $9° < 2\theta$. (b) Out-of-plane XRD profile of the LB film with 21 layers after immersion in the aqueous PbI_2/HI (0.5 mM/1.0 mM) solution for 50 min, together with a simulated XRD pattern for a bulk single crystal of the 2D layered $(C_{18}H_{37}NH_3)_2PbI_4$ hybrid perovskite.[33] (c) Orthorhombic crystal structure of the 2D layered organic−inorganic $(C_{18}H_{37}NH_3)_2PbI_4$ hybrid perovskite viewed along the b axis.[33] Lead and iodine atoms are shown in green and yellow colors, respectively.

band at 486 nm coincides well with the principal absorption band previously reported for a spin-coated film of 2D layered $(C_{18}H_{37}NH_3)_2PbI_4$ hybrid perovskite.[12] However, for the spin-coated 2D layered $(C_{18}H_{37}NH_3)_2PbI_4$ film, a weak second band caused by a different polymorph of the film was also reported at a longer wavelength.[12] For our system, a second band, similar to that observed by Kore and Gardner,[12] is not detected, indicating the homogeneity of the films fabricated in this study. The absorption and PL spectra of our films suggest that an excitonic band is formed in our thin system. This result is consistent with the previously reported bulk crystals and thin films of 2D layered $(C_nH_{2n+1}NH_3)_2PbI_4$ hybrid perovskite systems,[16−20] wherein 2D sheets of the inorganic PbI_6 octahedra and those of alkyl ammonium were alternately stacked to form QW superlattices.

Figure 3a shows the typical out-of-plane XRD profiles obtained before and after immersing the 21-layered ODA LB films in the aqueous solution of PbI_2/HI. The XRD profile of the as-deposited film exhibits distinct peaks at 2θ = 1.68, 5.09,

and 8.47°, which are in good agreement with those observed in earlier studies on Y-type ODA LB films.[31] The peaks at 2θ = 1.68, 5.09, and 8.47° can be assigned to the (001), (003), and (005) planes. The d-spacing of the as-deposited ODA LB film is 5.2 nm.[31]

The XRD profile of the films drastically changes after immersion. The three peaks at 2θ = 1.68, 5.09, and 8.47° disappear, and 12 new and distinct peaks emerge at 2θ = 2.78, 5.52, 8.23, 10.99, 13.75, 16.55, 19.28, 22.07, 24.86, 27.73, 30.54, and 33.42°, as shown in Figure 3a. Figure 3b also shows the same XRD profile of the LB film after immersion, together with a simulated XRD pattern for a bulk single crystal of the 2D layered $(C_{18}H_{37}NH_3)_2PbI_4$ hybrid perovskite.[33] The layered structure of the bulk single crystal viewed along the b axis is shown in Figure 3c. The crystal system is orthorhombic with a space group of $Pbca$ (61) (D_{2h}^{15}) (Z = 4) with a = 0.87825(1), b = 0.85401(1), c = 6.4472(11) nm, β = 90°, and U = 4.83376(11) nm^3.[19]

The organic layers of alkyl ammonium and inorganic lead iodide octahedra are stacked to form QW superlattices. Because the unit cell has a bilayer-like structure along the c axis, the interlayer spacing of the inorganic lead iodide tetrahedra is one half of lattice constant c.

The positions of the 12 peaks in the out-of-plane XRD pattern of the LB film after immersion coincided well with the simulated XRD peaks for $(0\ 0\ l)$ (l = 2, 4, 6, 8, 10, 12, 14, 16, 18, 20, 22, and 24), as shown in Figure 3b. Notably, the XRD pattern with peaks corresponding to only the $(0\ 0\ l)$ (l = 2, 4, 6, 8, 10, 12, 14, 16, 18, 20, 22, and 24) reflections indicates that the structure of our thin film after intercalation is equivalent to that of the corresponding $(C_{18}H_{37}NH_3)_2PbI_4$ single crystal, as schematically shown in Figure 3c, and that the c axis is vertically oriented with respect to the substrate surface. In other words, organic and inorganic layers are aligned parallel to the substrate surface. Note that the reflection of X-rays occurs only when l is even, if the structure of the film after immersion is equivalent to that of the $(C_{18}H_{37}NH_3)_2PbI_4$ single crystal based on the reflection conditions for an orthorhombic crystal with a space group of $Pbca$.[34] Furthermore, it is worth mentioning that the orientational order is fairly high, considering the higher-order reflections.

Therefore, it is probable that the corner-sharing PbI_6 octahedra are intercalated in the ODA LB films to form a well-organized $(C_{18}H_{37}NH_3)_2PbI_4$ thin film, associated with the protonation of the nitrogen atoms in the ODA molecules, as schematically shown in Figure 4. We hypothesize that the
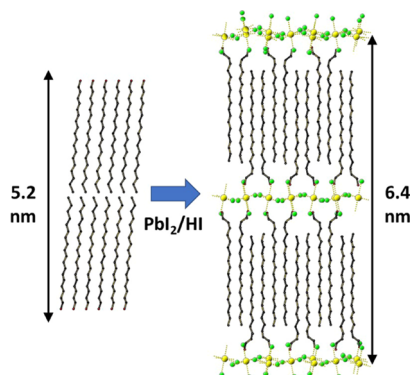
Figure 4. Schematic of the intercalation process. Nitrogen atoms of ODA molecules are protonated, and the lead iodide octahedral layers are intercalated to neutralize the positive charge.

structure of our intercalated thin films is equivalent to that of the corresponding $(C_{18}H_{37}NH_3)_2PbI_4$ single crystal, as illustrated in Figure 3c. The XRD analyses reveal that two different d-spacing values (d = 5.2 and 6.4 nm) could coexist in the LB film when the immersion time is less than 18 min (Figure S1). However, d = 5.2 nm, which is deduced for the as-deposited ODA LB film, disappears later (when the immersion time is more than 18 min), indicating the homogeneity of the resulting film. The intercalation mechanism is further verified using FT-IR spectroscopy data as explained later in this section.

Figure 5 shows the UV–visible absorption spectra of the ODA LB films with various numbers of layers (3, 7, 11, 15, and 21 layers) after immersing them in the aqueous solution of PbI_2/HI for 50 min. As shown in the inset, the peak absorbance at 486 nm increases in proportion to the number of layers, indicating that the layer-by-layer transfer of the
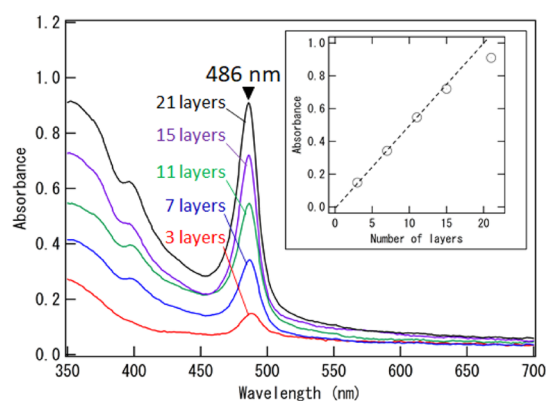
Figure 5. UV–visible absorption spectra of the ODA LB films with various numbers of layers after immersing them in the aqueous solution of PbI_2/HI for 50 min. The inset shows the absorbance peak at 486 nm plotted against the number of layers.

floating ODA layers onto the substrates is reproducible and that intercalation successfully proceeds irrespective of their thicknesses.

Figure 6 shows a typical fluorescence microscopy image of the ODA LB film after the immersion of the sample in the
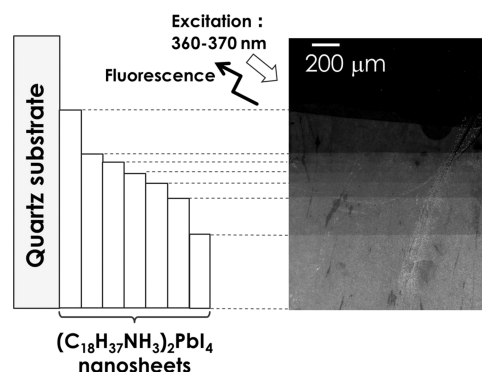
Figure 6. Typical fluorescence microscopy image of the ODA LB film (21 layers) after immersing it in the aqueous solution of PbI_2/HI for 50 min. The step structure was illuminated with UV light of 360−370 nm, and the PL image was obtained while blocking unwanted spectral components (<410 nm) using an optical filter set.

aqueous solution of PbI_2/HI for 50 min; the sample was illuminated with UV light of 360−370 nm. Nanometer-scale step structures can be often formed naturally by lowering of the air/water interface due to evaporation of water during the LB film deposition. The fluorescence image was obtained at such an area with the nanometer-scale step structure. As shown in Figure 6, a step structure is evident, reflecting the step structure created in the base material (ODA LB film). The gradual increase in brightness along the steps and the uniformity indicate that the proposed technique can facilitate a precise control on the thickness of the 2D layered $(C_{18}H_{37}NH_3)_2PbI_4$ hybrid perovskite, although some scratched and peeled areas can be recognized.

Note that the intercalation process results in an exciton band at 486 nm, even when the number of layers of the ODA LB film is only 3. PL was also confirmed by fluorescence microscopy as for the sample. Because the unit cell of the 2D layered $(C_{18}H_{37}NH_3)_2PbI_4$ hybrid perovskite has a bilayer-like structure (the interlayer spacing is one half of the unit cell

length along the c axis, as shown in Figure 4), the intercalated thin film can have only one QW structure when the number of layers in the ODA LB film is 3. In other words, the proposed technique can enable the fabrication of organized thin films of the 2D layered $(C_{18}H_{37}NH_3)_2PbI_4$ hybrid perovskite while controlling the number of QWs starting from single QW.

Figure S2 depicts the peak absorbance at 486 nm plotted against the immersion time of the LB films with various numbers of layers. Although the intercalation reaction seems almost over after 50 min regardless of the film thicknesses, the kinetics appears slower when the number of ODA layers is more than 11. We postulate that there should be a certain limit for fabricating thicker films. The studies to optimize intercalation conditions for thicker samples are in progress.

Figure 7 shows the typical FT-IR spectra in the wavenumber range of 2700−3450 cm^{-1} for the 21-layered ODA LB film
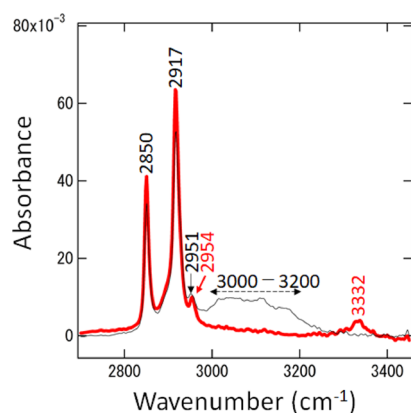
Figure 7. Transmission FT-IR spectra of the 21-layered ODA LB film before (thick solid line) and after immersion (thin solid line) in the aqueous PbI$_2$/HI solution.

before and after immersion in the aqueous PbI$_2$/HI solution. The thick solid line represents the spectrum of the as-deposited ODA LB film, whereas the thin solid one represents that after immersing it for 50 min. The spectrum of the as-deposited film has a broad and somewhat weak peak at 3332 cm^{-1}. A weak N−H stretching band of the aliphatic primary amine is located in this wavenumber region. For instance, the N−H stretch of octylamine, which is a hydrogen-bonded coupled doublet, occurs at 3290 and 3372 cm^{-1}, which can be assigned to the NH$_2$ symmetric (ν_sNH_2) and asymmetric ($\nu_{as}NH_2$) stretching bands, respectively.[35] Although the weak band observed at 3332 cm^{-1} can be assigned to either ν_sNH_2 or $\nu_{as}NH_2$ of ODA, further investigations for the assignment are currently in progress.

After the immersion of the LB film in the PbI$_2$/HI solution, the band at 3332 cm^{-1} disappears and a broad band appears in the wavenumber range of 3000−3200 cm^{-1}.[35] Primary amine salts exhibit a strong and broad absorption in the 2800−3200 cm^{-1} range, which can be assigned to the asymmetric and symmetric NH$_3^+$ stretching bands.[36,37] The strong band observed in the 3000−3200 cm^{-1} range can be ascribed to the asymmetric and symmetric N−H stretching bands of the NH$_3^+$ groups, which should appear owing to the protonation of the nitrogen atoms of the ODA molecules in the LB film when it is immersed in the PbI$_2$/HI solution. Although the assignment of the fine structure of the band is not straightforward, the broad band in the 3000−3200 cm^{-1}

range agrees well with that reported for a 2D layered lead iodide hybrid perovskite thin film, both in terms of position and shape, indicating the formation of alkyl ammonium salts.[38]

Based on the FT-IR spectra and XRD profile analyses, we can assume that the ODA molecules in the LB film are protonated in the aqueous PbI$_2$/HI solution and that the inorganic layers of the PbI$_6$ octahedra are intercalated in the organic layers of octadecyl ammonium to neutralize the positive charge, as schematically shown in Figure 4.

Both the spectra of the as-deposited (thick solid line) and intercalated (thin solid line) LB films show two distinct peaks at 2850 and 2917 cm^{-1}, which can be assigned to the CH$_2$ symmetric (ν_sCH_2) and asymmetric ($\nu_{as}CH_2$) stretching bands, respectively. Furthermore, the spectrum of the as-deposited LB film exhibits a small peak at 2954 cm^{-1}, which shifts to 2951 cm^{-1} after the intercalation; both these peaks can be attributed to the asymmetric CH$_3$ stretching bands ($\nu_{as}CH_3$).

The peak positions of ν_sCH_2 and $\nu_{as}CH_2$ are sensitive to the conformations of the hydrocarbon chains.[25,39−41] For example, when a hydrocarbon chain is in a solid crystalline state with an all-trans conformation, the ν_sCH_2 and $\nu_{as}CH_2$ bands are observed at 2848 and 2918 cm^{-1}, respectively. In contrast, when a hydrocarbon chain is in an isotropic (liquid) state, containing gauche forms, the $\nu_{as}CH_2$ and ν_sCH_2 bands are obtained at 2926 and 2856 cm^{-1}, respectively. The upward shift of the two bands ($\nu_{as}CH_2$ and ν_sCH_2) indicates an increase in the number of gauche conformers in hydrocarbon chains. Therefore, the peak positions are suitable indicators for evaluating the order of hydrocarbon chains.[25,39−41]

As shown by the thick and solid lines in Figure 7, the peak positions of the ν_sCH_2 and $\nu_{as}CH_2$ bands of the as-deposited LB film occur at 2850 and 2917 cm^{-1}, respectively. This result is consistent with that for hydrocarbons in all-trans conformations. Takahashi et al.[31] reported that the tilt angle of the hydrocarbon chain of the ODA LB film is 4.5°, which was estimated from the transmission and reflection−absorption FT-IR spectra.[31] However, the tilt angle of the chain is 3.4°, if we assume that the structure of the film is equivalent to that of the bulk single crystal of the 2D layered $(C_{18}H_{37}NH_3)_2PbI_4$ perovskite and that the c axis is vertically oriented with respect to the substrate surface, as shown in Figure 4.[19] Presently, studies are in progress to determine the orientation of hydrocarbon chains in these thin films, before and after intercalation, using infrared p-polarized multiangle incidence resolution spectrometry.[42,43] The corresponding results will be published elsewhere.

3. CONCLUSIONS

We demonstrated the fabrication of a well-organized thin film of the 2D layered $(C_{18}H_{37}NH_3)_2PbI_4$ hybrid perovskite by immersing the ODA LB films in an aqueous solution of PbI$_2$/HI (0.5 mM/1.0 mM). The immersed films exhibited a sharp absorption band at 486 nm (2.55 eV), and the growth of the band stabilized after 50 min of immersion. The immersed area exhibited a bright green emission under UV light (365 nm) at room temperature. The PL spectrum exhibited a distinct peak at 497 nm (2.50 eV) and was a mirror image of the absorption spectrum.

The XRD analyses indicate that the structure of the LB film after the immersion is equivalent to that of a room-temperature structural phase of the bulk single crystal of the $(C_{18}H_{37}NH_3)_2PbI_4$ perovskite, in which 2D layers of the lead

iodide octahedra and those of octadecyl ammonium are alternately stacked to form a QW structure.[1] Furthermore, only intense peaks of the $(0\,0\,l)$ (l = 2, 4, 6, 8, 10, 12, 14, 16, 18, 20, 22, and 24) reflections were observed in the out-of-plane XRD patterns, indicating that the c axis was vertically oriented with respect to the substrate surface. The observation of the higher-order reflections up to $(0\,0\,24)$ also indicates that the orientational order is remarkably high.

The absorbance of the exciton band located at 486 nm (2.55 eV) increases in proportion to the number of layers of the LB film, indicating that the number of QWs can be controlled layer-by-layer starting from 1. The fluorescence microscopy observation revealed that the surface of the film was uniform, reflecting the layer-by-layer deposition of the ODA LB film (base material). The FT-IR spectra indicated that the ODA molecules in the film were protonated in the aqueous PbI_2/HI solution and that the inorganic layers of the PbI_6 octahedra were intercalated in the alkyl ammonium film to neutralize the positive charge.

Based on all these data, we can conclude that the present technique enables the fabrication of well-organized thin films of 2D layered $(C_{18}H_{37}NH_3)_2PbI_4$ perovskite with a QW superlattice. Because the preparation conditions of the ODA LB film have been well established and the intercalation technique can be applicable to a wide range of metal cations and halogen anions, we believe that this technique will be beneficial in research on 2D layered organic−inorganic hybrid perovskite materials.

4. METHODS

4.1. Chemicals.
The film-forming compound, ODA $(CH_3(CH_2)_{18}NH_2)$ (GC grade ≥99.0%), was purchased from Sigma-Aldrich Co. LLC. Chloroform (GC grade ≥99.0%), used as the spreading solvent, was purchased from FUJIFILM Wako Pure Chemical Corporation. The basic subphase was prepared by dissolving NaOH (FUJIFILM Wako Chemicals, ≥96.0%; 1.4 mM) in pure water (PURELAB Flex UV). Lead(II) iodide (>98%) and hydriodic acid (55−58%, mass/mass), used for intercalation, were purchased from Tokyo Chemical Industry Co., Ltd. and FUJIFILM Wako Chemicals, respectively. All these chemicals were used without further purification.

4.2. LB Film Fabrication.
Prior to the spreading of the solution, the substrate (glass, fused quartz, and Si wafer) was partially immersed in the aqueous subphase using a clip, and the ODA/chloroform solution (1.0 mM) was applied dropwise at the air/water interface. After leaving the ODA for 5 min at the air/water interface, the film was compressed by applying a pressure of up to 50 mN/m and then transferred onto the substrate using the LB technique, in which an LB trough (Takahashi Seiki Co. Ltd., Type: Tycoon) was used. The dipping speed was 5 mm/min for the upward and downward strokes, and the transfer ratio was unity. During the entire fabrication process, the pH and temperature of the subphase were maintained in the ranges of 9.8−10.2 and 19−23 °C, respectively. Prior to the LB film deposition, the surface pressure−area per molecule isotherms were measured and confirmed to be coincident with those reported in previous studies,[3] indicating that an organized monomolecular film was formed at the air/water interface (Figure S3). An LB trough (NIMA Technology Ltd., Type: 622) was used for the surface pressure−area per molecule isotherm measurement.

A substrate with the dimensions of 1 mm × 13 mm × 38 mm or 1 mm × 8 mm × 38 mm, cut from a glass slide (Type S1111, Matsunami Glass Ind. Ltd., Japan), was used for the UV−visible absorption spectroscopy and XRD measurements. A fused quartz substrate with the dimensions of 1 mm × 13 mm × 38 mm (Sprasil P-30, Ohyo Koken Kogyo Co. Ltd., Japan) was used for the UV−visible absorption spectroscopy, fluorescence spectroscopy, and XRD measurements. An Si substrate with a dimension of 0.68 mm × 13 mm × 38 mm, cut from a Si wafer (both sides polished, <100>, p-type, contained B as the dopant; Valqua FFT Inc.), was used for transmission FT-IR spectroscopy. Prior to use, the glass and quartz substrates were soaked overnight in a KOH-saturated (Sigma-Aldrich Co. LLC, ≥86.0%) ethanol solution and used immediately after rinsing with pure water. The Si substrate was cleaned by sonication in isopropyl alcohol and used immediately after rinsing with chloroform.

4.3. Intercalation Procedure.
A cylindrical glass tube (inner diameter: 16 mm; depth: 45 mm) or a conventional rectangular UV quartz cuvette was filled with an aqueous PbI_2/HI (0.5 mM/1.0 mM) solution at 19−23 °C, and the as-deposited ODA LB films were immersed in the solution for 1−50 min.

4.4. Characterization.
The UV−visible absorption spectra were measured at 25 °C using a Shimadzu UV 1650 PC or Thermo Spectronic 200 spectrometer. The PL spectra were measured at 25 °C using a Hitachi F-7100 fluorescence spectrophotometer with an excitation wavelength of 350 nm. The fluorescence microscopy image was obtained using an Olympus IX83 inverted microscope with an optical filter set, by which the sample was illuminated with UV light of 360−370 nm, blocking unwanted spectral components (<410 nm). Transmission FT-IR absorption spectra were measured at 25 °C using a JASCO FT/IR-300 spectrometer. The spectrometer was purged with dry nitrogen gas to reduce absorption due to water vapor. Nonpolarized normal incident light was transmitted through the as-deposited and intercalated ODA LB films. To obtain a high signal-to-noise ratio, the spectra were recorded at a resolution of 4 cm^{-1} by co-adding 256 scans. The out-of-plane XRD analyses were performed using a Rigaku SmartLab X-ray diffractometer with Cu K$_\alpha$ radiation (λ = 0.15418 nm) (X-ray tube voltage and current: 45 kV and 200 mA, respectively) and a Rigaku MiniFlex diffractometer with Cu K$_\alpha$ radiation (λ = 0.15418 nm) (X-ray tube voltage and current: 30 kV and 15 mA, respectively). The structural data of the corresponding bulk single crystal of $(C_{18}H_{37}NH_3)_2PbI_4$ were downloaded from the Cambridge Crystallographic Data Centre[31] in the CIF format, and the powder XRD simulation was performed using commercial software (CrystalDifftract Ver.6.93, CrystalMaker Software Ltd.).

■ ASSOCIATED CONTENT

Ⓢ Supporting Information
The Supporting Information is available free of charge at https://pubs.acs.org/doi/10.1021/acsomega.2c05626.

> Out-of-plane XRD profiles of the 21-layered ODA LB film after immersion in the aqueous PbI_2/HI (0.5 mM/ 1.0 mM) solution for 30 s, 1 min, 2 min, 9 min, and 18 min, the peak absorbance at 486 nm of the ODA LB films with various numbers of layers plotted against durations for which the LB films were immersed in the PbI_2/HI (0.5 mM/1.0 mM) solution, and the surface

pressure−area per molecule isotherm of ODA measured at 19 °C (PDF)

Movies of the thin-film sample (21-layered ODA LB film after immersing it in the aqueous PbI_2/HI solution for 50 min under the irradiation of UV light) (MP4)

■ AUTHOR INFORMATION

Corresponding Author

Yasuhiro F. Miura − *Department of Physics, Hamamatsu University School of Medicine, Hamamatsu, Shizuoka 431-3192, Japan;* orcid.org/0000-0001-9479-9180; Phone: +81-(0)-53-435-2315; Email: yfmiura@hama-med.ac.jp

Authors

Yoshiya Akagi − *Department of Physics, Hamamatsu University School of Medicine, Hamamatsu, Shizuoka 431-3192, Japan*

Daizo Hishida − *Department of Materials & Life Sciences, Faculty of Science and Engineering, Sophia University, Tokyo 102-8554, Japan*

Yuko Takeoka − *Department of Materials & Life Sciences, Faculty of Science and Engineering, Sophia University, Tokyo 102-8554, Japan;* orcid.org/0000-0003-4958-3879

Complete contact information is available at:
https://pubs.acs.org/10.1021/acsomega.2c05626

Notes

The authors declare no competing financial interest.

■ REFERENCES

(1) Jena, A. K.; Kulkarni, A.; Miyasaka, T. Halide perovskite photovoltaics: background, status, and future prospects. *Chem. Rev.* **2019**, *119*, 3036−3103.

(2) Smith, M. D.; Connor, B. A.; Karunadasa, H. I. Tuning the luminescence of layered halide perovskites. *Chem. Rev.* **2019**, *119*, 3104−3139.

(3) Tian, W.; Zhou, H.; Li, L. Hybrid organic−inorganic perovskite photodetectors. *Small* **2017**, *13*, No. 1702107.

(4) Kishimoto, S.; Shibuya, K.; Nishikido, F.; Koshimizu, M.; Haruki, R.; Yoda, Y. Subnanosecond time-resolved X-ray measurements using an organic−inorganic perovskite scintillator. *Appl. Phys. Lett.* **2008**, *93*, 26191.

(5) Kawano, N.; Koshimizu, M.; Okada, G.; Fujimoto, Y.; Kawaguchi, N.; Yanagida, T.; Asai, K. Scintillating organic−inorganic layered perovskite-type compounds and the gamma-ray detection capabilities. *Sci. Rep.* **2017**, *7*, 14754.

(6) Zhang, H.; Hu, Y.; Wen, W.; Du, B.; Wu, L.; Chen, Y.; Feng, S.; Zou, C.; Shang, J.; Fan, H. J.; Yu, T. Vertical-cavity surface-emitting lasers based on 2D layered organic−inorganic hybrid perovskites. *APL Mater.* **2021**, *9*, No. 071106.

(7) Liu, T.; Zhao, X.; Li, J.; Liu, Z.; Liscio, F.; Milita, S.; Schroeder, B. C.; Fenwick, O. Enhanced control of self-doping in halide perovskites for improved thermoelectric performance. *Nat. Commun.* **2019**, *10*, 5750.

(8) Haque, M. A.; Kee, S.; Villalva, D. R.; Ong, W. L.; Baran, D. Halide perovskites: thermal transport and prospects for thermoelectricity. *Adv. Sci. (Weinh).* **2020**, *7*, No. 1903389.

(9) Mitzi, D. B. Introduction: perovskites. *Chem. Rev.* **2019**, *119*, 3033−3035.

(10) Zheng, K.; Pullerits, T. Two dimensions are better for perovskites. *J. Phys. Chem. Lett.* **2019**, *10*, 5881−5885.

(11) Takeoka, Y.; Mitzi, D. B. Halide perovskite materials, structural dimensionality, and synthesis. In *Perovskite Photovoltaics and Optoelectronics: From Fundamentals to Advanced Applications*, Miyasaka, T., Ed.; Wiley-VCH Verlag GmbH, 2021; 61−79.

(12) Kore, B. P.; Gardner, J. M. Water-resistant 2D lead(II) iodide perovskites: correlation between optical properties and phase transitions. *Mater. Adv.* **2020**, *1*, 2395−2400.

(13) Kim, B.; Seok, S. I. Molecular aspects of organic cations affecting the humidity stability of perovskites. *Energy Environ. Sci.* **2020**, *13*, 805−820.

(14) Kore, B. P.; Zhang, W.; Hoogendoorn, B. W.; Safdari, M.; Gardner, J. M. Moisture tolerant solar cells by encapsulating 3D perovskite with long-chain alkylammonium cation-based 2D perovskite. *Commun. Mater.* **2021**, *2*, 100.

(15) Chen, Y.; Yu, S.; Sun, Y.; Liang, Z. Phase engineering in quasi-2D Ruddlesden−Popper perovskites. *J. Phys. Chem. Lett.* **2018**, *9*, 2627−2631.

(16) Dolzhenko, Y. I.; Inabe, T.; Maruyama, Y. In situ X-ray observation on the intercalation of weak interaction molecules into perovskite-type layered crystals $(C_9H_{19}NH_3)_2PbI_4$ and $(C_{10}H_{21}NH_3)_2CdCl_4$. *Bull. Chem. Soc. Jpn.* **1986**, *59*, 563−567.

(17) Ishihara, T.; Takahashi, J.; Goto, T. Exciton state in two-dimensional perovskite semiconductor $(C_{10}H_{21}NH_3)_2PbI_4$. *Solid State Commun.* **1989**, *69*, 933−936.

(18) Ishihara, T.; Takahashi, J.; Goto, T. Optical properties due to electronic transitions in two-dimensional semiconductors $(C_nH_{2n+1}NH_3)_2PbI_4$. *Phys. Rev. B* **1990**, *42*, 11099−11107.

(19) Billing, D. G.; Lemmerer, A. Synthesis, characterization and phase transitions of the inorganic−organic layered perovskite-type hybrids $[(C_nH_{2n+1}NH_3)_2PbI_4]$ (n = 12, 14, 16 and 18). *New J. Chem.* **2008**, *32*, 1736−1746.

(20) Rademeyer, M.; Kruger, G. J.; Billing, D. G. Crystal structures and phase transitions of long-chain n-alkylammonium bromide monohydrates. *CrystEngComm* **2009**, *11*, 1926−1933.

(21) Tanaka, K.; Takahashi, T.; Kondo, T.; Umebayashi, T.; Asai, K.; Ema, K. Image charge effect on two-dimensional excitons in an inorganic−organic quantum-well crystal. *Phys. Rev. B* **2005**, *71*, No. 045312.

(22) Ema, K.; Inomata, M.; Kato, Y.; Kunugita, H.; Era, M. Nearly perfect triplet-triplet energy transfer from wannier excitons to naphthalene in organic−inorganic hybrid quantum-well materials. *Phys. Rev. Lett.* **2008**, *100*, No. 257401.

(23) Liang, K.; Mitzi, D. B.; Prikas, M. T. synthesis and characterization of organic−inorganic perovskite thin films prepared using a versatile two-step dipping technique. *Chem. Mater.* **1998**, *10*, 403−411.

(24) Takeoka, Y.; Fukasawa, M.; Matsui, T.; Kikuchi, K.; Rikukawa, M.; Sanui, K. Intercalated formation of two-dimensional and multi-layered perovskites in organic thin films. *Chem. Commun.* **2005**, *3*, 378−380.

(25) Myrzakozha, D. A.; Hasegawa, T.; Nishijo, J.; Imae, T.; Ozaki, Y. Structural characterization of Langmuir−Blodgett films of octadecyldimethylamine oxide and dioctadecyldimethylammonium chloride. 2. Thickness dependence of thermal behavior investigated by infrared spectroscopy and wetting measurements. *Langmuir* **1999**, *15*, 3601−3607.

(26) Miura, Y. F.; Akiyama, H.; Sugimoto, N.; Akagi, Y.; Aoyama, T.; Shiroishi, H.; Takahashi, M. Spherulitic crystallization in langmuir-blodgett films of the ditetradecyldimethylammonium-Au(dmit)$_2$ salt. *Langmuir* **2020**, *36*, 554−562.

(27) Era, M.; Oka, S. PbBr-based layered perovskite film using the Langmuir-Blodgett technique. *Thin Solid Films* **2000**, *376*, 232−235.

(28) Era, M.; Shimizu, A. PbI-based layered perovskite organic-inorganic superlattice film by the Langmuir−Blodgett technique. *Mol. Cryst. Liq. Cryst. Sci. Technol. Sect. A* **2001**, *370*, 215−218.

(29) Era, M.; Takada, N. Squeezed-out technique to prepare high-quality PbBr-based layered perovskite Langmuir-Blodgett films applicable to cavity polariton devices. *Langmuir* **2019**, *35*, 12224−12228.

(30) Ulman, A. *An Introduction to Ultrathin Organic Films from Langmuir-Blodgett to Self-Assembly*; Academic Press: New York, 1991; 107−132.

(31) Takahashi, M.; Kobayashi, K.; Takaoka, K.; Takada, T.; Tajima, K. Adsorption behavior and structural characterization of azo dyes on a Langmuir−Blodgett film of octadecylamine. *Langmuir* **2000**, *16*, 6613−6621.

(32) Honda, Z.; Fukuda, T.; Kamata, N. Intercalated formation of organic−inorganic hybrids based on the layered perovskite framework in organic Langmuir-Blodgett films. *J. Illum. Engng. Inst. Jpn.* **2009**, *93*, 794−797.

(33) Cambridge Crystallographic Data Centre (CCDC) (Deposition Number: 692957). http://www.ccdc.cam.ac.uk/structures (accessed 2022-04-15).

(34) International Tables for Crystallography, 6th ed.; *Space-Group Symmetry, Volume A*, Aroyo, M. I., Ed.; Wiley, 2016; 352−353.

(35) Silverstein, R. M.; Bassler, G. C.; Morrill, T. C. *Spectronic Identification of Organic Compounds*; Wiley: New York, 1991; 123−125.

(36) Colthup, N. B.; Daly, L. H.; Wiberley, S. E. *Introduction to Infrared and Raman Spectroscopy*; 3rd ed; Academic Press: New York, 1990; 339−344.

(37) Brissette, C.; Sandorfy, C. Hydrogen bonding in the amine hydrohalides: II. The infrared spectrum from 4000 to 2200 cm^{-1}. *Can. J. Chem.* **1960**, *38*, 34−44.

(38) Ishii, A.; Miyasaka, T. Direct detection of circular polarized light in helical 1D perovskite-based photodiode. *Sci. Adv.* **2020**, *6*, eabd3274.

(39) Umemura, J.; Cameron, D. G.; Mantsch, H. H. A Fourier transform infrared spectroscopic study of the molecular interaction of cholesterol with 1,2-dipalmitoyl-sn-glycero-3-phosphocholine. *Biochim. Biophys. Acta* **1980**, *602*, 32−44.

(40) Sapper, H.; Cameron, D. G.; Mantsch, H. H. The thermotropic phase behavior of ascorbyl palmitate: an infrared spectroscopic study. *Can. J. Chem.* **1981**, *59*, 2543−2549.

(41) Morita, S.; Iriyama, K.; Ozaki, Y. Aging effects on molecular orientation, structure, and morphology in Langmuir−Blodgett studied by infrared and ultraviolet−visible spectroscopy and atomic force microscopy. *J. Phys. Chem. B.* **2000**, *104*, 1183−1190.

(42) Hasegawa, T. A novel measurement technique of pure out-of-plane vibrational modes in thin films on a nonmetallic material with no polarizer. *J. Phys. Chem. B.* **2002**, *106*, 4112−4115.

(43) Hasegawa, T.; Shioya, N. MAIRS: innovation of molecular orientation analysis in a thin film. *Bull. Chem. Soc. Jpn.* **2020**, *93*, 1127−1138.